Unusual Field Dependence of the Anomalous Hall Effect in Ta/Tb-Fe-Co

M.D. Davydova,[1,2] P.N. Skirdkov,[1,3] K.A. Zvezdin,[1,3,*] Jong-Ching Wu,[4] Sheng-Zhe Ciou,[4]
Yi-Ru Chiou,[4] Lin-Xiu Ye,[5] Te-Ho Wu,[5] Ramesh Chandra Bhatt,[5] A.V. Kimel,[6] and
A.K. Zvezdin[3]

[1] *Moscow Institute of Physics and Technology, Dolgoprudny 141701, Russia*

[2] *Massachusetts Institute of Technology, 77 Massachusetts Ave, Cambridge, Massachusetts 02139, USA*

[3] *Prokhorov General Physics Institute of the Russian Academy of Sciences, Moscow 119991, Russia*

[4] *Department of Physics, National Changhua University of Education, Changhua 500, Taiwan*

[5] *Graduate School of Materials Science, National Yunlin University of Science and Technology, Douliu,
Yunlin 640, Taiwan*

[6] *Institute for Molecules and Materials, Radboud University, Nijmegen 6525 AJ, Netherlands*

Experimental studies of the anomalous Hall effect are performed for thin-film Ta/Tb-Fe-Co over a wide
range of temperatures and magnetic fields up to 3 T. Far from the compensation temperature ($T_M = 277$ K),
the field dependence has a conventional shape of a single hysteresis loop; just below the compensation
point, the dependence is anomalous with the shape of a triple hysteresis. To understand this behavior, we
experimentally reveal the magnetic phase diagram and theoretically analyze it in terms of spin-flop-like
phase transitions. In this case, we observe the dominance of the Fe-Co sublattice, which is a subject of the
strong interaction with the Ta layer. This Fe-Co anisotropy enhancement is expressed in the appearance of
abnormal wing-shaped hysteresis loops near the compensation point and, in the unusual phase diagram,
where the first-order phase transition line deviates towards low temperatures. This effect can be useful for
the design of ultrafast ferrimagnetic devices with desired switching parameters.

DOI: 10.1103/PhysRevApplied.13.034053

I. INTRODUCTION

Rare-earth/transition-metal (RE-TM) amorphous alloys and intermetallics form a wide class of ferrimagnetic materials that are particularly interesting in spintronics [1,2], optospintronics [3], ultrafast magnetism [4,5], and magnonics [6]. One of their biggest advantages is the sensitivity of their magnetic and transport properties to a subtle change of the composition, temperature, or application of magnetic field. Gd-Fe-Co and Tb-Fe-Co amorphous alloys are particular examples of such materials, and they have become model systems in ultrafast magnetism [7–11]. In these compounds, $4f$ rare-earth (Gd, Tb) is coupled antiferromagnetically to the $3d$ transition-metal (Fe-Co) sublattice. Magnetization of sublattices have different temperature dependencies. Therefore, by changing the concentrations of $4f$ and $3d$ elements in the compound, the compensation temperature, at which the magnetizations of the sublattices are mutually equal and the net magnetization is zero, can be tuned over a wide range of temperatures, including room temperature [12]. At temperatures lower than the compensation temperature,

the magnetization of the rare-earth (Tb) sublattice M_f is larger than that of the transition-metal (Fe-Co) M_d, while for temperatures above the compensation point $M_f < M_d$. Ultrafast magnetization reversal in RE-TM materials is demonstrated at record-breaking rates across the compensation temperature [13,14]. Also, in the vicinity of the compensation temperature, a relatively low magnetic field can turn the ferrimagnet into a noncollinear phase, in which the magnetic sublattices are canted and the net magnetization emerges [15]. Noncollinear spin configurations in ferrimagnets give rise to the anomalous Hall effect (AHE) [16]. This effect has been studied for more than a century [17]. Synergy between experimental and theoretical efforts in this area allow for the development of techniques for electrical detection of such subtle magnetic phenomena as dynamics of individual skyrmions [18]. In future, one may expect a further increase in the sensitivity of AHE detection through thermal fluctuations, as in the case of the spin-chirality-related Hall effect [19].

Here, we reveal, through the AHE-based technique, some unusual properties of a ferrimagnetic compound in the vicinity of the compensation temperature. Earlier experimental studies on Tb(Fe$_x$Co$_{1-x}$) [20,21], Gd(Fe$_x$Co$_{1-x}$) [15,22–25], Ho-Co [26], and DyCo$_4$ [27]

———————
*konstantin.zvezdin@gmail.com

demonstrated rather unusual behavior of the magnetization in these compounds. Unlike a single hysteresis loop, which is normally expected in measurements of the magnetization as a function of applied magnetic field, triple hysteresis loops are observed. Unlike our reports on triple hysteresis observed in pure Tb-Fe-Co just above the compensation temperature, T_M [21], here the situation is inverted such that the triple hysteresis is observed below T_M. More particularly, using Hall bar structures of MgO/Ta/Tb-Fe-Co, we measure the field dependencies of the anomalous Hall effect at various temperatures, with special focus on the domain in the vicinity of the compensation temperature. We experimentally define the magnetic phase diagram and propose a model that can explain this inversion. We show theoretically that the effect can result from an enhanced magnetic anisotropy of the d sublattice. Such an enhancement can originate from the Ta layer, which is known for a strong spin-orbit interaction. Thus, by changing the structure of the layered system, one can significantly influence the shape of the magnetic phase diagram. We suggest that our findings are relevant from a fundamental point of view, as well as for designing alternative RE-TM-based memory and spintronic devices with desired magnetic properties.

II. EXPERIMENTAL TECHNIQUE AND MEASUREMENT RESULTS

Multilayers of MgO(4 nm)/Ta(5 nm)/Tb-Fe-Co(10 nm)/SiO$_2$-coated Si (100) are prepared by means of a high-vacuum magnetron sputtering method. The magnetic Tb$_{28.5}$(Fe$_{80}$Co$_{20}$)$_{71.5}$ (the composition is identified using inductively coupled plasma mass spectrometry) layer is fabricated using cosputtering of an Fe-Co target and a Tb target. The sputtering power on each target is controlled for fine-tuning of the Tb concentration. No thermal annealing is performed. The Hall bar is fabricated as follows: (1) standard photolithography is employed to delineate the pattern of outer electrodes and probing pads; an ion-beam sputtering system equipped with two ion guns is then adopted for depositing copper film after using the second ion gun to etch the 4 nm MgO film on the top of the Ta/Tb-Fe-Co bilayer; (2) electron beam lithography is used for defining the Hall bar-shaped device, followed by the ion-beam etching technique to transfer the Hall bar-shaped device. The schematic structure of the Hall bar is shown in Fig. 1(a), an optical microscopy image of the Hall bar device is shown in Fig. 1(b), and an alternating gradient magnetometer measurement of the magnetization loop of the film at room temperature is given in Fig. 1(c).

A dc Hall measurement is carried out in a physical property measurement system that is equipped with a superconducting magnet capable of applying s magnetic field perpendicular to the film plane.
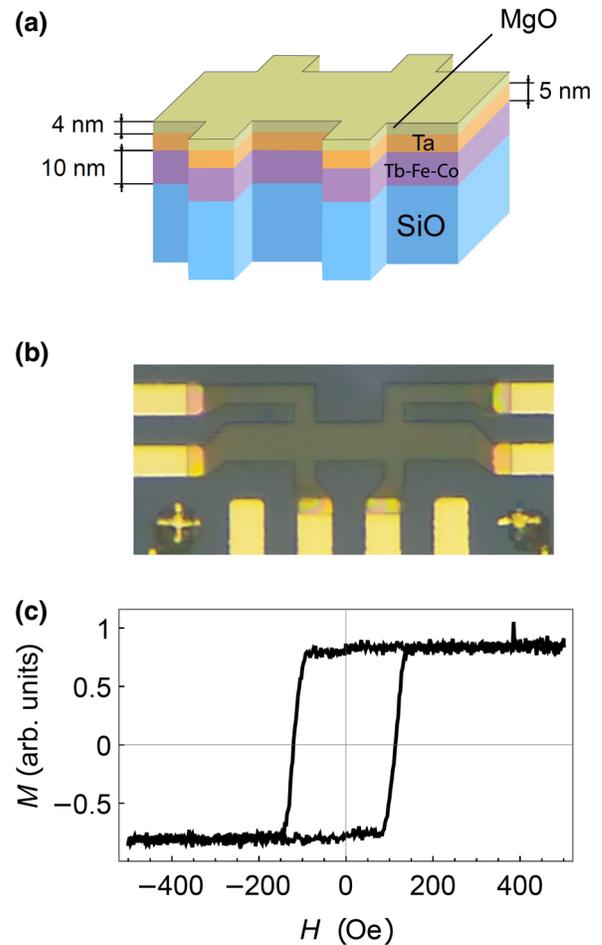

FIG. 1. (a) Scheme of structure with layers, (b) optical microscopy image of the Hall bar device. (c) Alternating gradient magnetometer measurement of magnetization loop of the film at room temperature.

We measure the dc AHE resistance at a sensing current of $I = 100 \, \mu$A to obtain the hysteresis curves of R_{AHE}, depending on the strength of the applied magnetic field, H, for a wide range of temperatures. The results of these measurements are shown in Fig. 2(a); the directions of sweeping are analogous to those indicated in Fig. 2(b). In Figs. 2(a) and 2(b), we see that the direction of the hysteresis loop inverts above the compensation temperature (for example compare curves at 263 and 283 K). Immediately below the compensation temperature, we observe anomalous behavior: triple hysteresis loops. They are shown for $T = 273$, 276.5, and 277 K in Fig. 2(a) and in more detail ($T = 271$, 272, 273, 274, and 276.5 K) in Fig. 2(b). The gray arrows indicate the edges of the hysteresis at positive fields and the blue arrows point to the second-order phase transition points. At the magnetization compensation temperature, T_M, the loops merge into one. We conclude that the magnetization compensation temperature, T_M, for the compound is between 276.5 and 277 K.
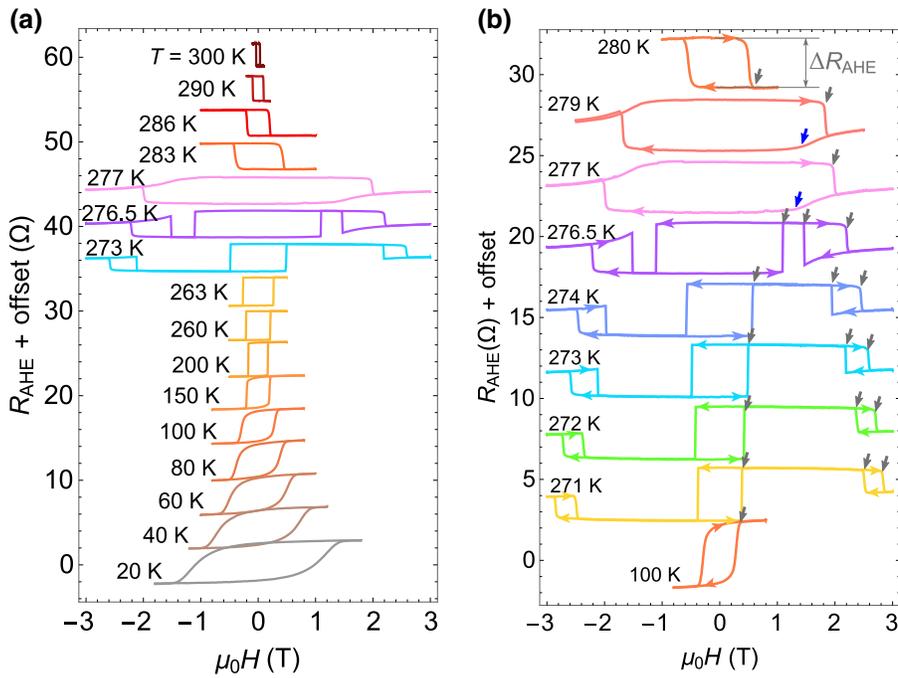
FIG. 2. Set of experimental AHE curves at different temperatures near the compensation point. The gray arrows indicate the edges of hysteresis at positive fields and the blue arrows point to the second-order phase transition points.

In Fig. 3(a), the hysteresis edges and spin-flop fields found using AHE measurements are shown for a wide range of temperatures. Gray diamonds correspond to the hysteresis edges that are illustrated by gray arrows in Fig. 2. Blue circles correspond to the spin-flop field [15] that is defined analogously to that in antiferromagnets [28].

Below it, the magnetizations of the sublattices are normal to the sample and directed oppositely. At the spin-flop field, the magnetizations become and form a noncollinear state. Examples of such transitions are located at the blue arrows in Fig. 2. The spin-flop transition is seen, for example, in Fig. 2 at $T = 277$ K as a bend at approximately 1.5 T, after which the magnetization curve becomes field-dependent. The growth of coercivity near 277 K confirms that this indeed is the compensation point.

In Fig. 3(b), the measured dependence of the height of the central hysteresis, ΔR_{AHE}, on temperature is shown. The sign flips at the compensation temperature. The AHE signal originates mostly from Fe-Co sublattice. This is why the resistivity changes sign at the compensation temperature where the sublattice magnetization flips.
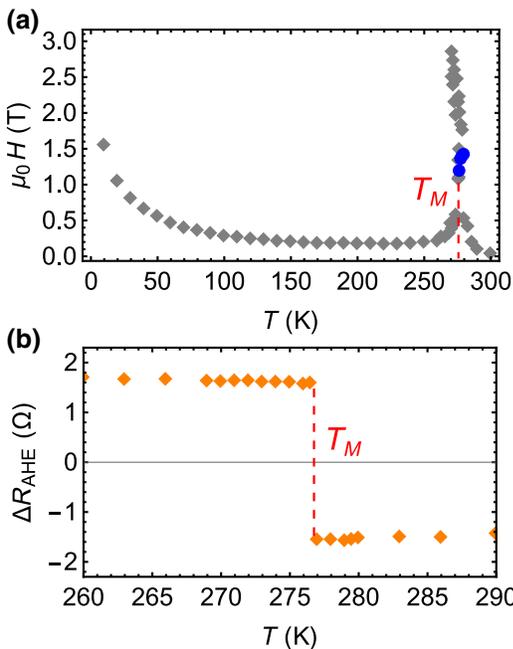

FIG. 3. Width, i.e., coercive field (a), and height, ΔR_{AHE} (b), of the central hysteresis loop of the anomalous Hall effect as functions of temperature. The compensation temperature is $T_M \approx 277$ K.

III. DISCUSSION

To examine the unusual behavior in more detail, we explore the peculiarities of the phase diagram in the vicinity of the compensation temperature. The left panel in Fig. 4 shows an experimentally defined H-T magnetic phase diagram of the studied Ta/Tb-Fe-Co structure. The right panel in Fig. 4 demonstrates three hysteresis curves at positive fields at (a) 273 K, (b) 279 K, and (c) 283 K. The magnetization orientations in each phase are shown schematically by arrows. Gray diamonds correspond to the edges of the hysteresis loops, and blue points correspond to the spin-flop transition points. The lines in the phase diagram are derived from the theoretical explanation that is similar to Refs. [21,29]. Similarly to our earlier reports,
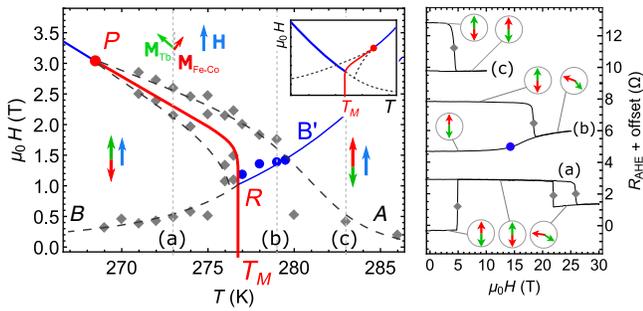
FIG. 4. Left: Experimentally measured features of the magnetic phase diagram near the compensation temperature. Gray and blue data points correspond to the edges of hysteresis and spin-flop fields, respectively. Orientation of magnetization vectors $\mathbf{M}_{Tb}$ and $\mathbf{M}_{Fe\text{-}Co}$ relative to external magnetic field $\mathbf{H}$ in different phases is shown schematically by green and red arrows, respectively. The lines are guides to the eye drawn according to theoretical predictions (see below in the Sec. III). Inset: typical shape of the Tb-Fe-Co phase diagram without Ta enhancement of Fe-Co anisotropy. Right: corresponding magnetization curves at (a) 273 K, (b) 279 K, and (c) 283 K. Data points corresponding to the phase diagram are shown by dots and diamonds. Magnetization orientation in different phases are shown schematically in circles.

here, we also interpret a hysteresis as a result of a first-order phase transition. If a change is gradual, it must be assigned to a second-order phase transition.

There are several phase transitions occurring in the magnetic phase diagram. We interpret the additional hysteresis loops to be a consequence of the first-order phase transition at high fields, which is always surrounded by hysteresis. The spin-flop points correspond to a second-order phase transition.

In the diagram, the solid blue lines (RB' and to the left from point P) and blue data points correspond to the second-order phase transition field. For temperature 273 K, AHE curve of which (b) is shown in the right panel in Fig. 4, the transition is indicated by a blue point. It occurs from a ferrimagnetic collinear (antiferromagnet-iclike) phase to a noncollinear one at a field strength of around 12 T. At this point, the sublattices become canted because of competition with antiferromagnetic exchange.

The gray dashed lines, BR, PR, and PA, in the phase diagram correspond to the lines of stability loss of different phases that surround the first-order transition lines between these phases. One first-order phase transition line is located at $H = 0$ and another one is indicated by the red line in Fig. 4. Point P is the tricritical point. Because of the additional first-order phase transition, $T_M RP$, that bends towards lower temperatures with an increase in magnetic field, there are anomalous hysteresis loops. An example of an AHE loop in the triple hysteresis regime is shown in curve (a) in the right panel of Fig. 4. If the system is initially in the energetically favorable ferrimagnetic phase,

in which the magnetization of Fe-Co sublattice is opposite to the external magnetic field, as it is supposed to be below, the compensation temperature, by sweeping the magnetic field, one will encounter a hysteresis at around 20–25 T. It occurs around the first-order phase transition to the noncollinear phase, where the sublattices are canted. By comparing curves (a) and (c) in Fig. 4, we can see that there is an inversion of the hysteresis loop at around $\mu_0 H = 0$ T.

The temperature range of the first-order phase transition analogous to $T_M RP$ in crystalline media is usually very small, of the order of less than 1 K [30]. Tb-Fe-Co is an amorphous alloy and, in this case, a sperimagnetic order [31] emerges near the phase transition points. In the sperimagnetic phase, there is a distribution of magnetic moments within a cone directed along the easy axis, which broadens the phase transitions, and thus, might be the reason behind an increased temperature range of this first-order phase transition up to 10 K in the experiment. The sperimagnetism of rare-earth/transition-metal compounds has been studied previously [31–36].

The above explanation of the phase diagram is based on the theory of a two-sublattice f-d ferrimagnet. Such theory employs a free energy that includes the intersublattice exchange interaction, Zeeman couplings of each sublattice, treats rare-earth ions in a paramagnetic approximation, and takes d-sublattice magnetization to be saturated by an intrasublattice exchange field. Below, we discuss only the most important distinctive feature of our study: the triple hysteresis loops. To explain the origin of the triple hysteresis loops, we can use a simplified model that allows this feature to be explained qualitatively; then we discuss the possible reasons why they occur below the compensation point in our experiment. For a description of the construction of the full phase diagram, we refer the reader to the relevant literature [21,30].

Below, we discuss the origin of the triple hysteresis and provide an explanation for why it occurs below the compensation temperature in this study. We use the free energy for a two-sublattice f-d (rare earth/transition metal) ferrimagnet with antiferromagnetic exchange that has the form [37]

$$F = -M_{Fe\text{-}Co}H\cos\theta_d - M_{Tb}[H^2 + (\lambda M_{Fe\text{-}Co})^2$$
$$- 2\,\lambda M_{Fe\text{-}Co}H\cos\theta_d]^{1/2} - K_u\cos^2\theta_d. \quad (1)$$

Here, θ_d is the polar angle defining the orientation of $\mathbf{M}_{Fe\text{-}Co}$; the first term is the Zeeman energy of the Fe-Co sublattice, which is saturated by large d-d exchange; the second term is the energy of the rare-earth sublattice in the effective field that is a sum of external field H and the intersublattice exchange field $H_{ex} = \lambda M_{Fe\text{-}Co}$. The last of these is usually in the order of 50 T [37]. The last term in Eq. (1) represents the anisotropy energy. The sublattices are coupled antiferromagnetically. K_u is the uniaxial

magnetic anisotropy constant that is a sum of several contributions: $K_u = -2\pi m^2 + K_{\text{Fe-Co}} + K_{\text{Tb}} + (2K_s/d)$. The first term is due to the demagnetizing field; $K_{\text{Fe-Co,Tb}}$ are the uniaxial anisotropy constants of the Fe-Co and Tb sublattices, respectively; and $2K_s/d$ is the surface anisotropy introduced by the Ta capping layer, depending on the total thickness of the film, d.

At the magnetization compensation point, T_M, the sublattice magnetizations are equal, $M_{\text{Tb}} = M_{\text{Fe-Co}}$. When H is less than H_{ex}, the most relevant term in the free energy is the anisotropy energy. The external magnetic field that is applied parallel to the easy magnetization axis leads only to renormalization of the anisotropy energy of the film. The energy can be written in the following form:

$$E_A \approx -\left(K_u - \frac{\chi_\perp H^2}{2} \right) \cos^2\theta, \qquad (2)$$

where θ is the polar angle defining the orientation of Neel vector $\mathbf{L} = \mathbf{M}_{\text{Fe-Co}} - \mathbf{M}_{\text{Tb}}$ (z axis is parallel to the normal to the film), $\chi_\perp$ is the perpendicular magnetic susceptibility, $\chi_\perp \approx (2M/H_{\text{ex}}) \gg \chi_\parallel$, $M = M_{\text{Fe-Co}} \approx M_{\text{Tb}}$. At the value of the magnetic field $H = H^* = (H_A H_{\text{ex}})^{1/2}$, the effective anisotropy constant $-[K_u - (\chi_\perp H^2/2)]$ changes sign, which leads to a phase transition. At the transition point, the angle θ changes in a jumplike fashion from π to $\pi/2$. $H_A = 2K_u/M$ is the anisotropy field.

Above, we see that, at the compensation temperature, $T = T_M$, the transition from the collinear to the noncollinear magnetic phase is of the first order, i.e., the order parameter experiences a jump. Let us now show how a first-order phase transition can occur at $T \neq T_M$. For certainty, consider $T < T_M$. At $T \neq T_M$, the sublattice magnetizations are not equal anymore and the Zeeman energy emerges. Near the compensation point in the linear order of H/H_{ex}, it has the form [37]

$$E_Z \approx -(M_{\text{Fe-Co}} - M_{\text{Tb}}) H \cos\theta. \qquad (3)$$

This interaction stabilizes the collinear phase where $\theta_d = \theta = \pi$. Due to competition between the Zeeman energy [Eq. (3)] and anisotropy energy [Eq. (2)], a noncollinear phase emerges near the compensation point that is described by the angle $\theta_d = \theta_{\text{NC}}(H, T \approx T_M)$, which is close to $\pi/2$. In a certain neighborhood of the compensation temperature at $T < T_M$ and $H \geq H^*$, there is an area where two phases, collinear $\theta_d = \theta_C = \pi$ and noncollinear $\theta_d = \theta_{\text{NC}}(H, T)$, coexist. The area is defined by the simultaneous satisfaction of the conditions of existence of the noncollinear phase and the collinear phases. The situation when two such solutions coexist is illustrated in Fig. 5. The possible phases correspond to the local minima of the free energy [Eq. (1)]. The phase transition between these two phases that occurs within this area is of the first order, which explains the observed triple hysteresis loops.
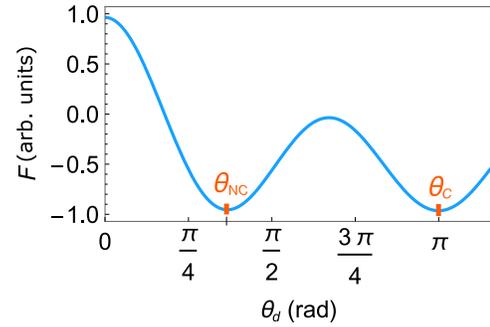

FIG. 5. Dependence of free energy [Eq. (1)] on the angle θ_d below the compensation temperature at $M_{\text{Tb}}/M_{\text{Fe-Co}} = 1.002$, $H_A = 0.01\,H_{\text{ex}}$, and $H = 0.1H_{\text{ex}}$, which corresponds to the vicinity of the first-order phase transition. Possible phases correspond to the minima of free energy. NC, noncollinear.

Lastly, let us discuss the temperature range of the triple hysteresis loops. For the case when the rare-earth anisotropy is prevailing, in contrast to the considered case of the dominance of the Fe-Co sublattice, which is a subject of the strong interaction with the Ta layer, we have shown earlier [21,37,38] that in similar systems an inclination towards higher temperatures should occur. In Ref. [21], where the magnetization curves were studied experimentally in Tb-Fe-Co without a Ta capping layer and an inclination of the first-order phase transition towards higher temperatures was observed, in contrast to the present results. Indeed, Fe-Co anisotropy enhancement by strong interaction with the Ta layer leads in our case to the appearance of triple hysteresis loops below the compensation temperature, while in case of Tb-Fe-Co without a Ta capping layer they appear above.

Since Tb usually possesses higher anisotropy than that of the d sublattice, one would expect such behavior in the present experiment. However, we observe that this is not a case. Earlier studies of rare-earth ferrimagnets, which are based on the free energy similar to Eq. (1), have found that, in the case of weak rare-earth magnetic anisotropy, the transition shifts towards lower temperatures with increasing magnetic field [39]. Therefore, one might assume that there is a source of enhancement of the magnetic anisotropy of the d sublattice in our study. Indeed, the surface anisotropy introduced by Ta capping influences d states that are relatively more delocalized, and thus, for Ta-coated Tb-Fe-Co, the f-sublattice anisotropy does not dominate, at least in the vicinity of the compensation temperature of the film. The physical reason behind this is that Ta, the electronic configuration of which is [Xe] $4f$ 14 $5d$3 $6s$2, has a large atomic number, $Z = 73$, and the spin-orbit coupling scales approximately as $Z4$ [40]. Therefore, due to Ta coating, the d subsystem of the material has increased magnetic anisotropy.

IV. CONCLUSIONS

Here, we report unusual hysteresis loops of the anomalous Hall effect in $Tb_{28.5}(Fe_{80}Co_{20})_{71.5}$ ferrimagnetic compound. From the experimental data, we deduce a magnetic phase diagram. We explain the hysteresis loops in terms of spin-flop-like phase transitions. It is shown that the anomalous hysteresis loops will take place below the magnetization compensation, if the magnetic anisotropy is dominated by the contribution from the transition-metal sublattice. In contrast to pure Tb-Fe-Co, the magnetic anisotropy experienced by the spins of the transition metal can be enhanced by the presence of the Ta capping layer, which is known for strong spin-orbit interactions. Our findings offer a way for the smart engineering of ferrimagnetic heterostructures with desired properties.

[1] S. D. Bader and S. S. P. Parkin, Spintronics, Annu. Rev. Condens. Matter Phys. **1**, 71 (2010).

[2] M. Nakayama, T. Kai, N. Shimomura, M. Amano, E. Kitagawa, T. Nagase, M. Yoshikawa, T. Kishi, S. Ikegawa, and H. Yoda, Spin transfer switching in TbCoFe/CoFeB/MgO/CoFeB/TbCoFe magnetic tunnel junctions with perpendicular magnetic anisotropy, J. Appl. Phys. **103**, 07A710 (2008).

[3] T. J. Huisman, C. Ciccarelli, A. Tsukamoto, R. V. Mikhaylovskiy, T. Rasing, and A. V. Kimel, Spin-photo-currents generated by femtosecond laser pulses in a ferrimagnetic GdFeCo/Pt bilayer, Appl. Phys. Lett. **110**, 072402 (2017).

[4] J.-Y. Bigot, M. Vomir, and E. Beaurepaire, Coherent ultrafast magnetism induced by femtosecond laser pulses, Nat. Phys. **5**, 515 (2009).

[5] A. Kirilyuk, A. V. Kimel, and T. Rasing, Ultrafast optical manipulation of magnetic order, Rev. Mod. Phys. **82**, 2731 (2010).

[6] D. Ghader, V. Ashokan, M. A. Ghantous, and A. Khater, Spin waves transport across a ferrimagnetically ordered nanojunction of cobalt-gadolinium alloy between cobalt leads, Eur. Phys. J. B **86**, 180 (2013).

[7] C. D. Stanciu, A. V. Kimel, F. Hansteen, A. Tsukamoto, A. Itoh, A. Kirilyuk, and T. Rasing, Ultrafast spin dynamics across compensation points in ferrimagnetic GdFeCo: The role of angular momentum compensation, Phys. Rev. B **73**, 220402 (2006).

[8] C. D. Stanciu, F. Hansteen, A. V. Kimel, A. Kirilyuk, A. Tsukamoto, A. Itoh, and T. Rasing, All-optical Magnetic Recording with Circularly Polarized Light, Phys. Rev. Lett. **99**, 047601 (2007).

[9] L. Le Guyader, M. Savoini, S. El Moussaoui, M. Buzzi, A. Tsukamoto, A. Itoh, A. Kirilyuk, T. Rasing, A. V. Kimel, and F. Nolting, Nanoscale sub-100 picosecond all-optical

[10] magnetization switching in GdFeCo microstructures, Nat. Commun. **6**, 5839 (2015).

[10] T.-M. Liu, *et al.*, Nanoscale confinement of all-optical magnetic switching in TbFeCo-competition with nanoscale heterogeneity, Nano Lett. **15**, 6862 (2015).

[11] J.-W. Kim, K.-D. Lee, J.-W. Jeong, and S.-C. Shin, Ultrafast spin demagnetization by nonthermal electrons of TbFe alloy film, Appl. Phys. Lett. **94**, 192506 (2009).

[12] R. Moreno, T. A. Ostler, R. W. Chantrell, and O. Chubykalo-Fesenko, Conditions for thermally induced all-optical switching in ferrimagnetic alloys: Modeling of TbCo, Phys. Rev. B **96**, 014409 (2017).

[13] C. D. Stanciu, A. Tsukamoto, A. V. Kimel, F. Hansteen, A. Kirilyuk, A. Itoh, and T. Rasing, Subpicosecond Magnetization Reversal Across Ferrimagnetic Compensation Points, Phys. Rev. Lett. **99**, 217204 (2007).

[14] Z. Chen, R. Gao, Z. Wang, C. Xu, D. Chen, and T. Lai, Field-dependent ultrafast dynamics and mechanism of magnetization reversal across ferrimagnetic compensation points in GdFeCo amorphous alloy films, J. Appl. Phys. **108**, 023902 (2010).

[15] J. Becker, A. Tsukamoto, A. Kirilyuk, J. C. Maan, Th. Rasing, P. C. M. Christianen, and A. V. Kimel, Ultrafast Magnetism of a Ferrimagnet Across the Spin-Flop Transition in High Magnetic Fields, Phys. Rev. Lett. **118**, 117203 (2017).

[16] J. Sinova, S. O. Valenzuela, J. Wunderlich, C. H. Back, and T. Jungwirth, Spin hall effects, Rev. Mod. Phys. **87**, 1213 (2015).

[17] N. Nagaosa, J. Sinova, S. Onoda, A. H. MacDonald, and N. P. Ong, Anomalous hall effect, Rev. Mod. Phys. **82**, 1539 (2010).

[18] D. Maccariello, W. Legrand, N. Reyren, K. Garcia, K. Bouzehouane, S. Collin, V. Cros, and A. Fert, Electrical detection of single magnetic skyrmions in metallic multilayers at room temperature, Nat. Nanotechnol. **13**, 233 (2018).

[19] Y. Kato and H. Ishizuka, Colossal Enhancement of Spin-Chirality-Related Hall Effect by Thermal Fluctuation, Phys. Rev. Appl. **12**, 021001 (2019).

[20] T. Chen and R. Malmhäll, Anomalous hysteresis loops in single and double layer sputtered TbFe films, J. Magn. Magn. Mater. **35**, 269 (1983).

[21] A. Pogrebna, K. Prabhakara, M. Davydova, J. Becker, A. Tsukamoto, T. Rasing, A. Kirilyuk, A. K. Zvezdin, P. C. M. Christianen, and A. V. Kimel, High-field anomalies of equilibrium and ultrafast magnetism in rare-earth–transition-metal ferrimagnets, Phys. Rev. B **100**, 174427 (2019).

[22] S. Esho, Anomalous magneto-optical hysteresis loops of sputtered Gd-Co films, Jpn. J. Appl. Phys. **15**, 93 (1976).

[23] K. Okamoto and N. Miura, Hall effect in a RE-TM perpendicular magnetic anisotropy film under pulsed high magnetic fields, Phys. B Condens. Matter **155**, 259 (1989).

[24] M. Amatsu, S. Honda, and T. Kusuda, Anomalous hysteresis loops and domain observation in Gd-Fe co-evaporated films, IEEE Trans. Magn. **13**, 1612 (1977).

[25] C. Xu, Z. Chen, D. Chen, S. Zhou, and T. Lai, Origin of anomalous hysteresis loops induced by femtosecond laser pulses in GdFeCo amorphous films, Appl. Phys. Lett. **96**, 092514 (2010).

[26] H. Ratajczak and I. Gošciaňska, Hall hysteresis loops in the vicinity of compensation temperature in amorphous HoCo films, Phys. Status Solidi **62,** 163 (1980).

[27] K. Chen, D. Lott, F. Radu, F. Choueikani, E. Otero, and P. Ohresser, Observation of an atomic exchange bias effect in $DyCo_4$ film, Sci. Rep. **5,** 18377 (2016).

[28] A. E. Clark and E. Callen, Néel ferrimagnets in large magnetic fields, J. Appl. Phys. **39,** 5972 (1968).

[29] M. D. Davydova, K. A. Zvezdin, J. Becker, A. V. Kimel, and A. K. Zvezdin, $H-T$ phase diagram of rare-earth–transition-metal alloys in the vicinity of the compensation point, Phys. Rev. B **100,** 064409 (2019).

[30] K. P. Belov, A. K. Zvezdin, and A. M. Kadomtseva, *Orientational Phase Transitions* (Nauka, Moscow, 1979).

[31] J. M. D. Coey, Amorphous magnetic order, J. Appl. Phys. **49,** 1646 (1978).

[32] G. V. Sayko, S. N. Utochkin, and A. K. Zvezdin, Spin-reorientation phase transitions in thin films of RE-TM amorphous alloys, J. Magn. Magn. Mater. **113,** 194 (1992).

[33] L. M. Garcia, S. Pizzini, J. P. Rueff, J. Vogel, R. M. Galera, A. Fontaine, J. B. Goedkoop, N. B. Brookes, J. P. Kappler, and G. Krill, The beamline ID24 at ESRF for energy dispersive X-ray absorption spectroscopy, Le J. Phys. IV **7,** C2 (1997).

[34] L. M. Garcia, S. Pizzini, J. P. Rueff, J. Vogel, R. M. Galéra, A. Fontaine, J. P. Kappler, G. Krill, and J. Goedkoop, Temperature and field-induced magnetization flips in amorphous $Er - Fe$ alloys evidenced by x-ray magnetic circular dichroism, J. Appl. Phys. **79,** 6497 (1996).

[35] S. Pizzini, L. M. Garcı́a, A. Fontaine, J. P. Rueff, J. Vogel, R. M. Galéra, J. B. Goedkoop, N. B. Brookes, G. Krill, and J. P. Kappler, Magnetic phase diagram of an amorphous $Er - Fe$ alloy studied by X-ray magnetic circular dichroism, J. Electron Spectros. Relat. Phenomena **86,** 165 (1997).

[36] A. R. Wildes and N. Cowlam, Sperimagnetism in $Fe_{78}Er_5B_{17}$ and $Fe_{64}Er_{19}B_{17}$ metallic glasses: I. Moment values and non-collinear components, J. Phys. Condens. Matter **23,** 496004 (2011).

[37] A. K. Zvezdin, Chapter 4 field induced phase transitions in ferrimagnets, Handb. Mag. Mater. **9,** 405 (1995).

[38] C. K. Sabdenov, M. D. Davydova, K. A. Zvezdin, A. K. Zvezdin, A. V. Andreev, D. I. Gorbunov, E. A. Tereshina, Y. Skourski, J. Šebek, and I. S. Tereshina, Magnetic properties of $HoFe_6Al_6$ with a compensation point near absolute zero: A theoretical and experimental study, J. Alloys Compd. **708,** 1161 (2017).

[39] A. K. Zvezdin and V. M. Matveev, Some features of the physical properties of rare-earth iron garnets near the compensation temperature, JETP **35,** 140 (1972).

[40] M. Blume, A. J. Freeman, and R. E. Watson, Theory of spin-orbit coupling in atoms. III, Phys. Rev. **134,** A320 (1964).